Journal of the Korean Nuclear Society
Volume 34, Number 2, pp.154~164, April, 2002

Neutron Cross Section Evaluation on Dy Isotopes

Y. D. Lee and J. H. Chang
Korea Atomic Energy Research Institute
150 Dukjin-dong, Yuseung-gu, Daejeon, Korea, 305-353
ydlee@nanum.kaeri.re.kr

(Received August 13, 2001)

Abstract

Neutron cross section data on Dy-160, Dy-161, Dy-162, Dy-163 and Dy-164 were calculated and evaluated in the energy range of 1 keV to 20 MeV using a spherical optical model, statistical model and pre-equilibrium model. The energy dependent optical model potential parameters were obtained based on the recent experimental data. The width fluctuation correction in Hauser-Feshbach particle decay and the quantum mechanical approach in pre-equilibrium analysis were introduced and gave a better cross section calculation in EMPIRE-II. The total, elastic scattering and threshold reaction cross sections were evaluated and compared with the evaluated files. The model calculated (n, tot), (n, γ) and (n, p) cross sections were in good agreement with the experimental data in the measured energy range. The results will be applied to ENDF/B-VI for data improvement.

Key Words : cross section, evaluation, optical model potential, EWDF/B-VI

I. Introduction

Dysprosium (Dy) is a material considered as a neutron absorber in nuclear fuel or in a reactor control rod. Dy isotopes are significant fission products as well in spent fuel. They have the feature that each isotope has a large capture cross section. Therefore, Dy can absorb neutrons continuously and effectively for a long term period. Table 1 summarizes the property and production of Dy isotopes in a fission reactor.

The capture cross sections of Dy isotopes are part of a comprehensive study of the rare earth region. This region is of special importance since the solar abundance of these chemically almost identical elements is known to be greater than 2%[1] and is, therefore, best suited for comparison with the s-process abundance predicted by various stellar models. The Dy-163 is an exotic case, where a terrestrially stable nucleus starts to decay in a stellar environment.

Dy-160, Dy-161, Dy-162, Dy-163 and Dy-164 were considered in the evaluation, having 2.34%, 18.9%, 25.5%, 24.9% and 28.2% respectively in natural abundance. The ENDF/B-VI was compiled for Dy-160, Dy-161, Dy-162 and Dy-163 in 1974 and for Dy-164 in 1967. Therefore, a new evaluation on neutron cross sections based on

Table 1. Dy Property and Production in Fission Reactor

Isotope	Property and Production	1st excited level
Dy-160	- stable - accumulated · by beta decay from Tb-160 · by electron capture from Ho-160 - negligible by direct fission from U-238, Pu-239	87 keV
Dy-161	- stable - mainly accumulated · by beta decay from Tb-161 · by electron capture from Ho-161 - negligible by direct fission from U-238, Pu-239	26 keV
Dy-162	- stable - mainly accumulated · by beta decay from Tb-162 · by electron capture from Ho-162 - negligible by direct fission from U-238, Pu-239	81 keV
Dy-163	- stable - mainly accumulated · by beta decay from Tb-163 · by electron capture from Ho-163 - produced by direct fission from U-238, Pu-239	73 keV
Dy-164	- stable - accumulated · by beta decay from Tb-164 · by electron capture from Ho-164 - produced by direct fission from U-238, Pu-239	73 keV

recent experiment data is necessary and important for better application.

Reference input parameter library (RIPL)[2] published by IAEA involves several different optical model potential shapes and corresponding parameters for many nuclides. However, the published potentials are limited in an incident neutron energy, target mass and proton number. Unfortunately, for Dy isotopes, the potentials in RIPL do not reproduce the total cross section properly to the recent experimental data[3]. Therefore, the potential search as a function of incident neutron energy is essential in the optical model. This potential provides the basis of the theoretical cross section generation on Dy isotopes. Moreover, the comparison of the s-wave strength functions between calculated by the potential parameters in the unresolved resonance region and estimated by the measurement in the resolved resonance region was made and was helpful in obtaining the calculated cross sections closer to the experimental data.

The cross sections were generated by nuclear models and the evaluation was done based on the reference experimental data. ABRXPL[4] was developed to search the energy dependent potential parameters. It controls ABAREX and displays the calculated total, elastic scattering and

capture cross sections on a screen to compare with the experimental data. Nuclear reaction cross sections were calculated by EMPIRE-II[5], having a Hauser-Feshbach model and a quantum mechanical approach using multistep direct (MSD) and multistep compound (MSC) in a pre-equilibrium energy range. EMPIRE-II involves the width fluctuation correction and the dynamic approach to level densities (including energy dependent in level density parameter). EMPIRE-II offers the ENSDF nuclear level library. The evaluated cross sections were (n, tot), (n, n), (n, n'), (n, γ), (n, p), (n, α), (n, 2n), (n, 3n), (n, nα) and (n, np). These were graphically compared with the experimental data and evaluated files (ENDF/B-VI and JEF-2.2). The evaluated results were compiled to ENDF-6 format and will improve ENDF/B-VI.

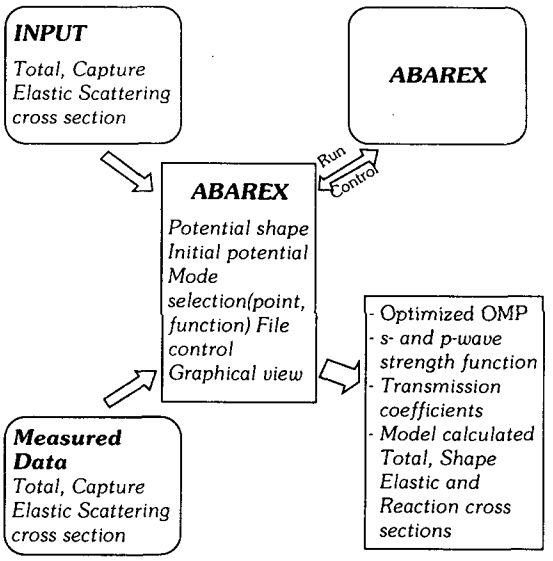

Fig. 1. OMP Searching Process in ABAREX

2. Optical Model

The optical model code, ABAREX[6], was used to provide the proper potential and transmission coefficients for cross section data generation. To obtain proper potential parameters, the Woods-Saxon well is used for the real optical model potential

$$V(r) = -V / \{1+\exp((r-R_v)/a_v)\} \quad (1)$$

where V and a_v are the strength and diffuseness of the potential, respectively, and the nuclear radius Rv, related to mass number A, is given by

$$R_v = r_v A^{1/3}. \quad (2)$$

The derivative Woods-Saxon shape is used for the imaginary part of the optical model potential.

$$W(r) = -4W \exp((r-R_w)/a_w) / \{1+ \exp((r-R_w)/a_w)\}^2 \quad (3)$$

where W, R_w and a_w are potential strength, radius and diffuseness respectively. Generally, Thomas form is taken in the optical model potential for spin-orbit coupling

$$V_{s\text{-}o}(r) = (2\overline{L} \cdot \overline{S})V_{so}(2/r)\{d/dr(1/ [1+\exp((r-R_{so})/a_{so})])\} \quad (4)$$

where $\overline{L} \cdot \overline{S}$ is the dot product of the orbital and spin angular momentum operator.

The spherical optical model potential depth and radius of real and imaginary parts were defined as a function of incident neutron energy,

$$V=V_o+V_1 \times E_n, \quad r_v = r_{vo} + r_{v1} \times E_n \quad (5a)$$

$$W=W_o + W_1 \times E_n, \quad r_w=r_{wo} + r_{w1} \times E_n \quad (5b)$$

where E_n is an incident neutron energy. The 13 potential parameters (V_o, V_1, r_{vo}, r_{v1}, a_v, W_o, W_1, r_{wo}, r_{w1}, a_w, V_{so}, r_{so}, a_{so}) were searched simultaneously based on the Voss' s total and capture experimental data[3]. Fig. 1 shows the schematic

Table 2. Selected Energy Dependent Optical Model Potential Parameters: 1 keV~20 MeV Incident Neutron Energy Range

Parameter	Dy-160	Dy-161	Dy-162	Dy-163	Dy-164
Vo(MeV)	47.0100	47.0178	46.0170	45.5100	46.5100
V1(MeV)	-0.267	-0.267	-0.267	-0.267	-0.267
rvo(fm)	1.2090	1.2699	1.1530	1.2400	1.1870
av(fm)	0.520	0.480	0.460	0.460	0.460
Wo(MeV)	9.920	13.12	11.32	9.920	10.52
rwo(fm)	1.2120	1.2416	1.1870	1.2410	1.1830
aw(fm)	0.540	0.640	0.740	0.560	0.640
Vso(MeV)	7.000	7.000	7.000	7.000	7.000
rso(fm)	1.2700	1.2699	1.2400	1.2698	1.2697
aso(fm)	0.660	0.660	0.660	0.660	0.660
W1(MeV)	-0.053	-0.053	-0.053	-0.053	-0.053
rw1(fm)	0.000	0.000	0.000	0.000	0.000
rv1(fm)	0.000	0.000	0.000	0.000	0.000

diagram of the potential parameter searching process and the obtainable outputs. The extracted potential parameters are summarized in Table 2. The potential depth of Dy isotopes for the real and imaginary part has a range from 45 MeV to 47 MeV and from 9 MeV to 13 MeV. The radius varies from 1.15 fm to 1.26 fm for the real part and from 1.18 fm to 1.24 fm for the imaginary one. The potential depth for the real part was not changed significantly in odd and even mass number Dy isotopes. Specially, for even and even cases (Dy-162 and Dy-164), the parameters were similar to those of others. The radius for real and imaginary parts did not varied much in Dy isotopes. However, Table 2 shows the relatively larger variation of the imaginary potential depth in each isotope. The similar parameters were obtained in the spin-orbit coupling part for all isotopes. The potential for spin-orbit coupling does not have much influence on neutron cross section data generation.

Transmission coefficient, $T_\ell = 1 - |\eta_\ell|^2$, is calculated by the search potential and used to calculate physical quantities such as total (σ_T), shape elastic (σ_E), and reaction (σ_R) cross sections as well as strength functions and scattering radius. For simplicity, if we neglect the spin of the neutron, the shape elastic scattering cross section is given by sum of the ℓ^{th} partial wave in the radial wave equation of the Schroedinger equation

$$\sigma_E = \pi/k^2 \sum_{\ell=0}^{\infty} (2\ell+1)|1-\eta_\ell|^2 \qquad (6)$$

where η_ℓ is the complex reflection factor and k is the number of waves. The reaction cross section is expressed as

$$\sigma_R = \pi/k^2 \sum_{\ell=0}^{\infty} (2\ell+1)(1-|\eta_\ell|^2) \qquad (7)$$

and the total cross section is defined by

$$\sigma_T = \pi/k^2 \sum_{\ell=0}^{\infty} (2\ell+1)[1-\Re(\eta_\ell)], \qquad (8)$$

Table 3. Comparison of the Calculated s-wave Strength Function (produced by ABAREX)

Isotopes	s-wavestrength function	
	By Optical Model	By evaluation
Dy-160	2.09×10^{-4}	$2.00 \times 10^{-4} \pm 0.40 \times 10^{-4}$
Dy-161	2.52×10^{-4}	$1.76 \times 10^{-4} \pm 0.17 \times 10^{-4}$
Dy-162	1.79×10^{-4}	$1.80 \times 10^{-4} \pm 0.30 \times 10^{-4}$
Dy-163	2.09×10^{-4}	$1.90 \times 10^{-4} \pm 0.30 \times 10^{-4}$
Dy-164	1.74×10^{-4}	$1.70 \times 10^{-4} \pm 0.25 \times 10^{-4}$

*By ABAREX at 1 keV

**Evaluation at resonance region[16]

where $\mathcal{R}$ is the real part of η_ℓ.

In the unresolved energy region, when target spin is zero, the s-wave strength function is calculated in ABAREX[6] by

$$S_o = (E_1/E)^{1/2}(\Gamma/D), \quad (9)$$

where Γ is the average width of an s-wave resonance, D is the average spacing between the resonances in the averaging interval, E is the average energy in the measurement interval and E_1 is the reference energy which is conventionally taken to be 1 eV. Table 3 shows S_o calculated at 1 keV energy from the selected potential parameters and evaluated from the resonance parameters. The calculated S_o follows the evaluated reference quite well, except Dy-161. S_o will help to match the model calculated total cross section with the produced by the resonance parameters in the unresolved region. Especially, when only a few experimental data exist for total and elastic cross sections, S_o plays an important role in cross section generation.

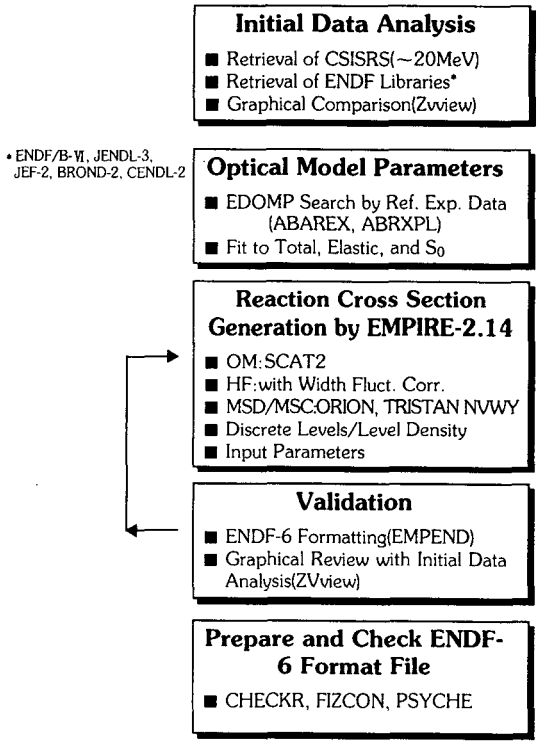

Fig. 2. Process for Cross Section Generation and Evaluation

3. Cross Section Generation

3.1. Process

Fig. 2 shows the whole process of nuclear data generation and evaluation. As a preliminary step, we retrieve and analyze the available experimental data and the evaluated files (ENDF/B-VI, JENDL-3, JEF-2, BROND-2 and CENDL-2). The searched potential is applied for total, elastic

scattering, reaction cross section data and transmission coefficient calculations up to 20 MeV energy range in EMPIRE-II. These data are used for the individual threshold reaction cross section calculation.

EMPIRE-II has several advantages for cross section data generation: width fluctuation correction in Hauser-Feshbach decay for particles and gamma rays, discrete levels matching in level densities, angular distribution of emitted particles from the compound, the quantum mechanical approach in pre-equilibrium analysis using MSD by Tamura-Udagawa-Lenske[7] and MSC by Nishioka-Verbaarschot-Weidenmuller-Yoshida[8], the pre-equilibrium exciton model with full angular momentum coupling, a complete gamma ray cascade after emission of each particle-including realistic treatment of gamma ray transitions between low-lying discrete levels and an easy graphical view of calculated cross sections with experimental data and evaluated files. The multi-step direct model in EMPIRE-II takes care of the inelastic scattering to vibrational collective levels and decay information. The evaluated files are checked by ENDF-VI format checking codes (CHECKR, FIZCON and PSYCHE).

The width fluctuation correction term in the cross section by Hauser-Feshbach is important to compound elastic scattering, inelastic scattering and capture cross section calculations. The width fluctuation correction term is introduced in the Hauser-Feshbach theory to take into account the correlations between the incident and outgoing waves in the decay channels. This may be done formally by defining the corrected cross section to be

$$\sigma^{HF} = \pi\lambda_\alpha^2 T_\alpha T_\beta W_{\alpha\beta} / \sum_i T_i \qquad (10)$$

where $W_{\alpha\beta}$ is the width fluctuation correction factor. This factor depends on the transmission

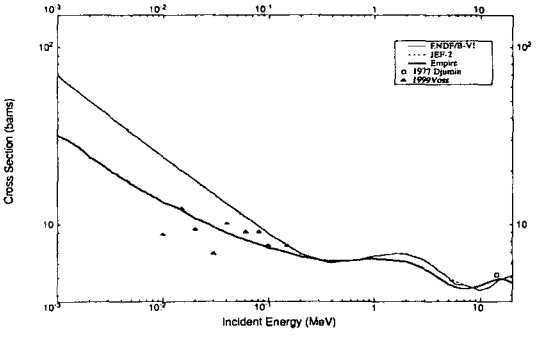

Fig. 3. Total Cross Section for Dy-160

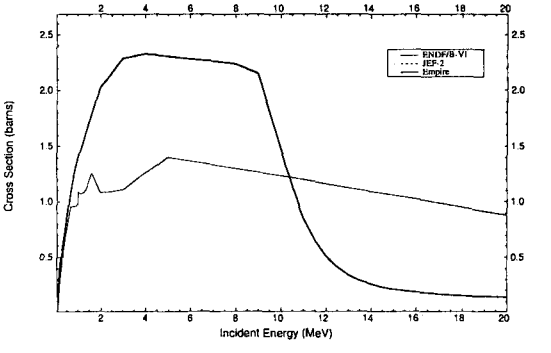

Fig. 4. (n,n') Cross Section for Dy-160

coefficients T_i. T_α and T_β are the transmission coefficients of a reaction channel α and a decay channel β. It is noted that the correction depends on the incident energy and falls rapidly with increasing energy, becoming negligible at energies of a few MeV. Therefore, the correction is important in the low energy region.

3.2. Calculations

In this paper, the selected cross sections, (n, tot), (n, n'), (n, γ) and (n, p), are discussed in the following figures, which are important reactions from 1 keV to 20 MeV. The calculated cross sections were compared with the experimental data and the evaluated files (ENDF/B-VI and JEF-2.2). Especially, the calculated total and capture

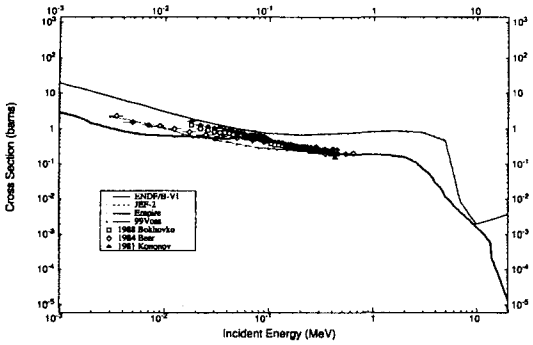

Fig. 5. (n,γ) Cross Section for Dy-160

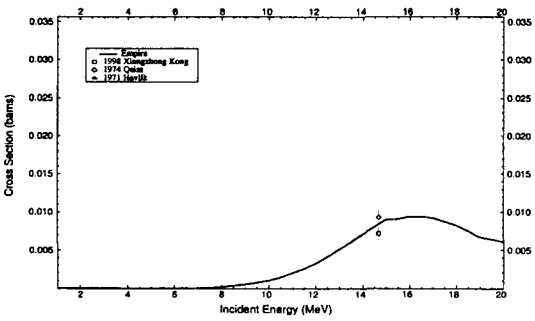

Fig. 6. (n, p) Cross Section for Dy-160

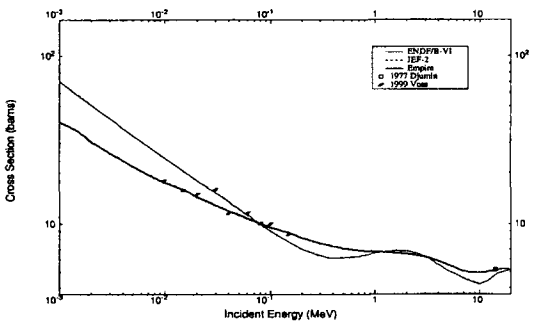

Fig. 7. Total Cross Section for Dy-161

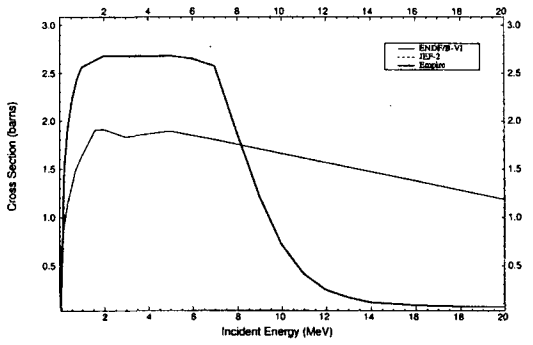

Fig. 8. (n, n') Cross Section for Dy-161

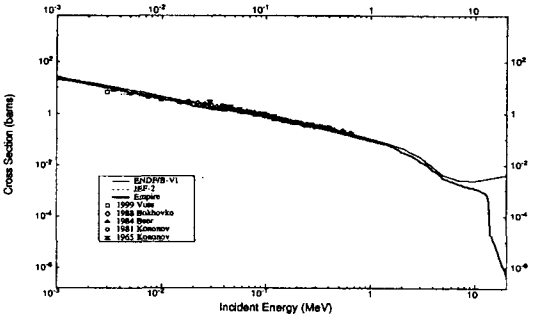

Fig. 9. (n, γ) Cross Section for Dy-161

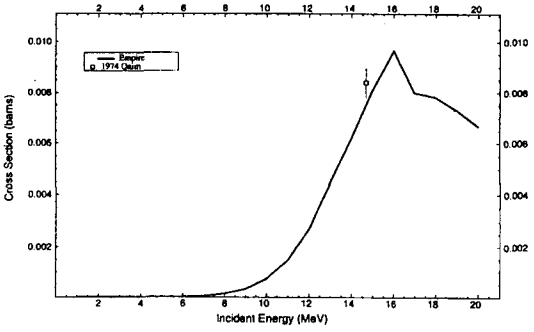

Fig. 10. (n, p) Cross Section for Dy-161

cross sections were compared with Voss et al.[3] reference. However, in the unresolved region overlapped from the resonance evaluation[18], resonance parameters will be used to produce the cross sections in the ENDF-6 formatted full set, until the 1st excited level energy.

Fig. 3 shows the comparison of the calculated result to the experimental data[3,9] and ENDF/B-VI for Dy-160. The model calculated total cross section by the searched optical model potential was in good agreement with the experimental data. However, in the measured energy range, the calculation is somewhat different from ENDF/B-VI. ENDF/B-VI is higher than Voss data. Fig. 4

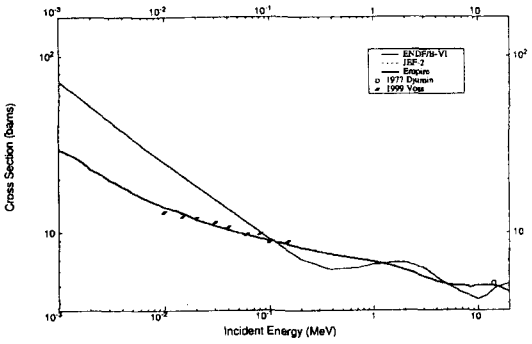

Fig. 11. Total Cross Section for Dy-161

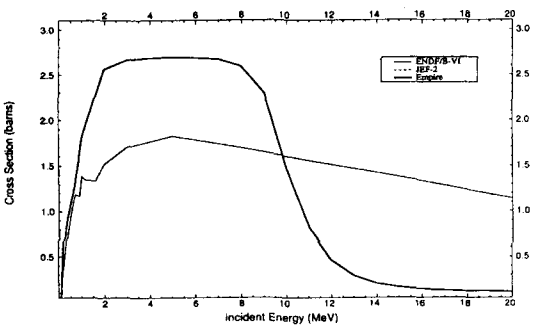

Fig. 12. (n, n') Cross Section for Dy-161

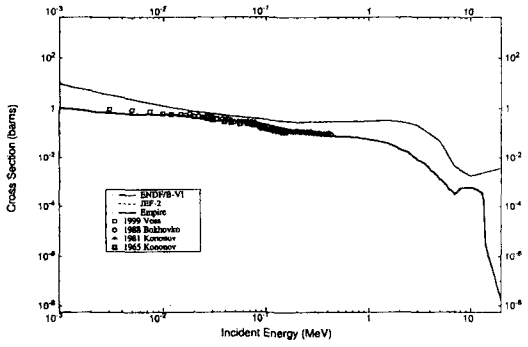

Fig. 13. (n, γ) Cross Section for Dy-162

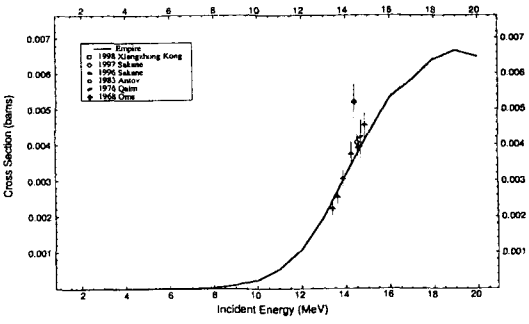

Fig. 14. (n, p) Cross Section for Dy-162

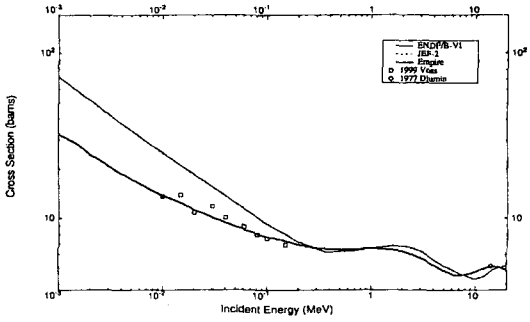

Fig. 15. Total Cross Section for Dy-163

shows the (n, n') cross section. There is no experimental data for (n, n'). Fig. 5 shows the (n, γ) cross section results. This capture cross section is very important as an absorbing material. ENDF/B-VI is always higher than the experimental data[3,10,11,12] in the measurement energy range. However, Fig. 5 shows good agreement between the calculation and the experimental data above the first excited level of Dy-160, 87 keV. However, below 40 keV, there is a difference between the calculation and the measured data, the calculation being lower than the experimental data and ENDF/B-VI. In this energy range, the capture cross section will be replaced by the resonance parameters. Fig. 6 is for the (n, p) cross section. The calculated result is in good agreement with the experimental data[13].

Fig. 7 shows the total cross section for Dy-161. The calculated result follows the experimental data[3,9] well in the measured energy range and 14 MeV. There is a slope difference in the low energy range between the calculation and the ENDF/B-VI. Below 70 keV, ENDF/B-VI is higher than the calculation. Fig. 8 is the (n, n') cross

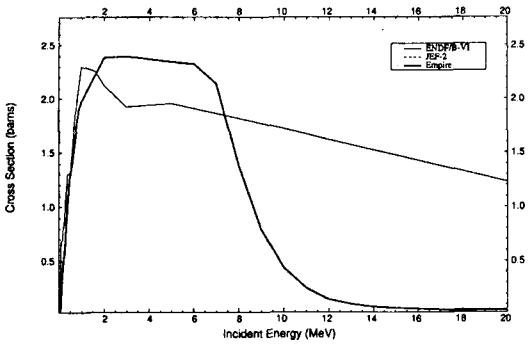

Fig. 16. (n,n') Cross Section for Dy-163

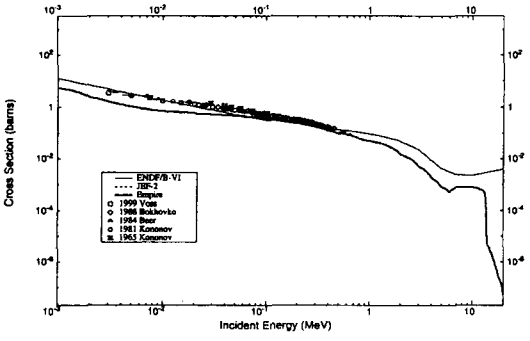

Fig. 17. (n, γ) Cross Section for Dy-163

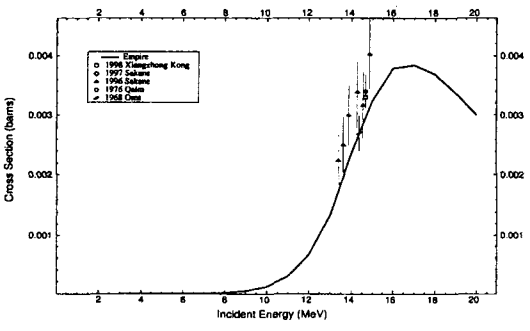

Fig. 18. (n, p) Cross Section for Dy-163

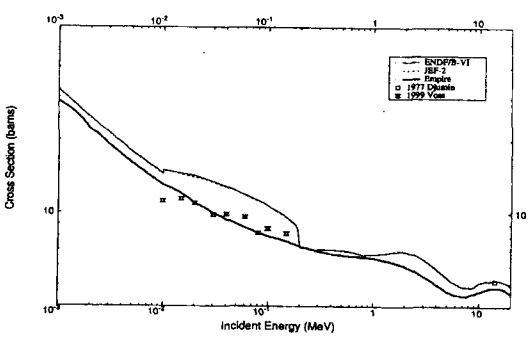

Fig. 19. (n, p) Cross Section for Dy-164

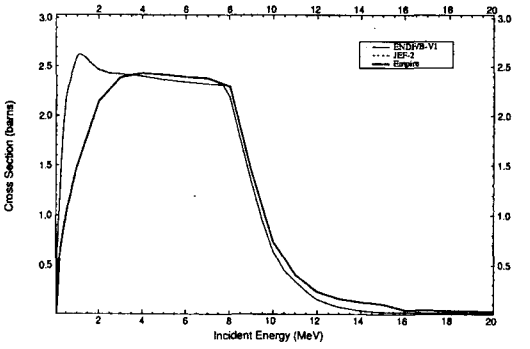

Fig. 20. (n, n') Cross Section for Dy-164

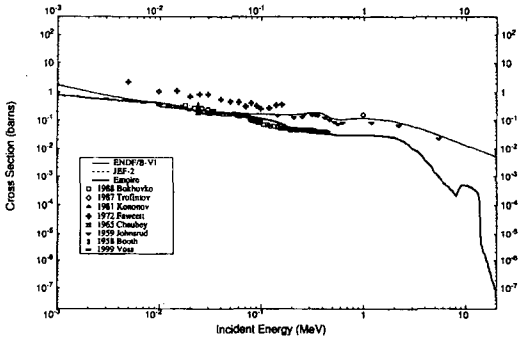

Fig. 21. (n, γ) Cross Section for Dy-164

section for Dy-161. Fig. 9 shows good agreement between the calculated (n, γ) cross section and the experimental data[3,10,11,12] and ENDF/B-VI agrees with the experimental data as well. Fig. 10 shows the (n, p) cross section. (n, p) cross section is close to Qaim data[13] at 14.7 MeV.

The comparison of the total cross section on Dy-162 was done in Fig. 11. The calculated total cross section was in very good agreement with the measured data. However, Fig. 11 shows the difference between the calculation and the ENDF/B-VI. Below 100 keV, ENDF/B-VI is

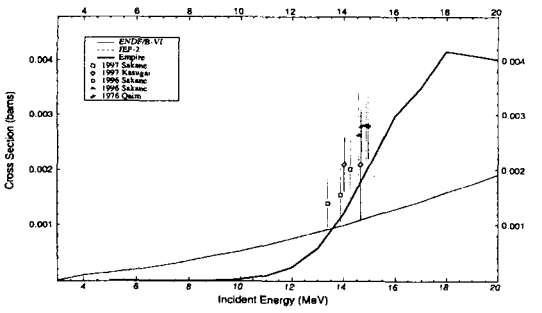

Fig. 22. (n, p) Cross Section for Dy-164

higher than the calculation. Fig. 12 is the (n, n') cross section. Fig. 13 shows the comparison of the (n, γ) cross section. In the whole evaluation energy range, ENDF/B-VI is higher than the experimental data and the calculated result. The calculated result follows the experimental data[3,10,12] well. The calculated (n, p) cross section was also in good agreement with the experimental data[13,17], as shown in Fig. 14.

Fig. 15 shows the total cross section of Dy-163. The calculated result is in good agreement with the experimental data. ENDF/B-VI is higher than the Voss data in the low energy. Fig. 16 shows the (n, n') cross section on Dy-163. Fig. 17 shows the (n, γ) cross section. The calculated capture cross section was in good agreement with the experimental data above 80 keV. The capture cross section below 80 keV will be replaced by the resonance parameters. The calculated (n, p) cross section shows good agreement with the experimental data[13,17] in Fig. 18.

Fig. 19 shows the total cross section between the calculated result and the ENDF/B-VI for Dy-164. ENDF/B-IV has an unusual shape from 10 keV to 150 keV in the figure. The calculation is in good agreement with the experimental data[3]. Fig. 20 shows the (n, n') cross section. Fig. 21 shows the (n, γ) cross section for Dy-164. The calculated result shows good agreement with the experimental data[3,10,11,12]. Above 60 keV figure shows the difference between the calculation and the ENDF/B-VI. ENDF/B-VI seems to follow the old experimental data[14,15]. Fig. 22 shows the calculated (n, p) cross section for Dy-164. The calculation seems to follow the experimental data[13,17] within the statistical fluctuation.

4. Conclusions

The extracted optical model potential parameters were functioned successfully in the measured energy range and in the whole evaluation energy range. ABRXPL was effective for obtaining the proper energy dependent optical model potential parameters. The evaluation process was enough to generate the total, elastic and threshold reaction cross sections. The calculated total and capture cross sections for Dy isotopes were in good agreement with the experimental data. However, the calculated total cross sections were different from the ENDF/B-VI in the whole evaluation energy range. Especially, in the low energy region, the slope was totally different from the ENDF/B-VI. The capture cross sections of Dy-160 and Dy-162 in ENDF/B-VI were higher than the calculated results. The current evaluations will improve the ENDF/B-VI.

Acknowledgements

This work is performed under the auspices of the Korea Ministry of Science and Technology as a long-term R&D project.

References

1. E. Anders and N. Grevesse, Geochim. Cosmochim. Acta 53, 197 (1989).
2. P. G. Young, Handbook for calculations of

nuclear reaction data reference library, Reference Input Parameter Library (RIPL), IAEA, (1998).

3. F. Voss et al, "Stellar Neutron Capture Cross Sections of Pr and Dy Isotopes," Physical Review C, Vol. 59, No. 2, 1154-1170, Feb, (1999).
4. Y. D. Lee, "ABRXPL development for parameter decision of spherical optical model potential," KAERI, NDL-14/99.
5. M. Herman, Empire-2:Statistical Model Code for Nuclear Reaction Calculations IAEA, Vienna, (2000).
6. R. D. Lawson, "ABAREX_A Neutron Spherical Optical-Statistical Model Code," in Workshop on Computation and Analysis of Nuclear Data Relevant to Nuclear Energy and Safety, pp447-516, Trieste, Feb. 10 - Mar. 13, 1992.
7. T. Tamura, T. Udagawa and H. Lenske, Phys. Rev. C26, 379 (1982).
8. H. Nishioka, J. J. M. Verbaarschot, H. A. Weidenmuller and S. Yoshida, Ann. Phys. 172 (1986).
9. A. N. Djumin, "Nuclear Radii for Some Isotopes Derived from Total Neutron Cross-Sections," C, Kiev, 2, 74, (1977).
10. V. N. Kononov et al, Fourth Int. Symp. On Neutron Capture Gamma-ray Spectroscopy and Related Topics, Sept. 7-11, Grenoble, EXFOR 40621.3-6, (1981).
11. H. Beer, G. Walter, "Neutron Capture Cross Sections and Solar Abundances of 160,161Dy, 170,171Yb, 175,176Lu, and 176,177Hf for the S-process Analysis of the Radionuclide 176Lu," Physical Review C, Vol. 30, No. 2, 464-478, Aug. (1984).
12. M. V. Bokhovko et al., "The Fast Neutron Radiation Capture for Dysprosium Isotopes," J, YK, (4), 8, (1988).
13. S. M. Qaim, "Precision Measurements and Sustematics of (n,2n) (n,p) and (n,a) Reaction Cross-Sections at 14.7 MeV," J, JIN, 35, 3669, (1973).
14. A. E. Johnsrud et al, "Energy Dependence of Fast-Neutron Activation Cross Section," J. of Phys. Rev. Vol.116(927), (1959).
15. L. R. Fawcett et al, "Neutron Capture Cross Sections in the keV Region for 154-Sm, 160-Gd, 164-Dy, and 165-Ho," Nucl. Sci. and Eng. Vol.49(317), (1972).
16. S.F. Mughabghab, Neutron Cross Sections, Vol.1, Part B, (1984).
17. H. Sakane et al., "Measurement of Formation Cross Section of Short-Lived Nuclei by 14 MeV Neutrons - Nd, Sm, Dy, Er, Yb," S, JAERI-97-004, 193, (1996).
18. S.Y. Oh et al., "Evaluation of Neutron Cross Sections of Dy Isotopes in the Resonance Region," J. of KNS, Vol.33, (1), 46-61, (2001).